

Assessing the Safety of a Velocity Sourced Series Elastic Actuator Using the Head Injury Criterion

Gordon Wyeth and Geoff Walker
School of Information Technology and Electrical Engineering
University of Queensland
{wyeth, walkerg}@itee.uq.edu.au

Abstract

The Velocity Sourced Series Elastic Actuator has been proposed as a method for providing safe force or torque based actuation for robots without compromising the actuator performance. In this paper we assess the safety of Velocity Sourced Series Elastic Actuators by measuring the Head Injury Criterion scores for collisions with a model head. The study makes a comparative analysis against stiff, high impedance actuation using the same motor without the series elastic component, showing that the series elastic component brings about a massive reduction in the chance of head injury. The benefits of a collision detection and safe reaction system are shown to be limited to collisions at low speeds, providing greater interaction comfort but not necessarily contributing to safety from injury.

1 Introduction

A dramatic rise in research and commercial interest in medical and service robotics has developed the new field of human-centred robotics. This field addresses the many challenges in creating close interactions between humans and robots, including direct contact between robots and humans. Current standards for robot safety prohibit such contact, and with good reason. Current robot technology is more than capable of killing; the first robot “homicide” was recorded in 1981 when factory worker Kenji Urada was killed by a robot after he inadvertently bypassed safety systems. The standards for robot safety specify failsafe robot enclosures that keep humans completely out of the robot’s workspace at all times. How then are we to move towards the vision of robots helping us in our homes and workplaces?

While robot safety must necessarily be addressed by a range of strategies, many researchers are focussing on reducing the inertia and stiffness of robot manipulators. Most robots use high impedance (stiff) position controlled actuators typical of industrial robot arms. When a high impedance robot collides with an obstacle, the forces rise dangerously due to the error in

position. A low impedance robot will sacrifice position to maintain a safe force level. Low impedance actuation means that the actuators source force (or torque) to the load, rather than commanding the load’s position (or angle). Torque control of a geared motor can reduce the impedance of actuation at low frequencies, but cannot completely remove the high moment of inertia of the motor seen through the gearbox which creates a high impact load. Direct drive technologies (where the motor drives the load without a gearbox) can reduce but not eliminate this problem, and lead to much heavier and more voluminous solutions. At higher frequencies above the control bandwidth, the mechanical impedance of either actuator is still very high. The magnitudes of impact loads, which are determined by inertia and stiffness of the interface, are not attenuated.

The Series Elastic Actuator (SEA) deliberately introduces compliance via a spring between the motor-gearbox and the load, and so has intrinsic low impedance. Our previous work has shown that it is feasible to produce high performance from an SEA while retaining the inherent safety given by the actuator’s low effective inertia and stiffness [1]. The improvement in performance was principally achieved having tight velocity control of the DC motor that acts as the mechanical power source for the actuator.

The paper shows that our variant of the SEA, the Velocity Sourced SEA, is intrinsically safe by a series of quantitative measurements of the Head Injury Criteria (HIC) [2], a standard used in automotive safety. The paper reviews the principles of the Velocity Sourced SEA, and then gives quantified results for its safety against a high impedance actuator system. The paper illustrates the value of implementing a system of collision detection and safe reaction. The paper goes on to quantify the likelihood of injury using the Abbreviated Injury Scale [3].

2 Velocity Sourced SEA

The SEA principle has been investigated for over a decade ([4],[5],[6],[7]), but has struggled to deliver high torque bandwidth. In our previous work, we changed the paradigm for SEA design by treating the motor as a

velocity source rather than as a torque source (see Figure 1). This idea is suggested in [8]. The reason that this idea becomes attractive is that a tight velocity control loop on the motor can overcome some of the undesirable effects of the motor and the gearbox. Velocity control is also more straightforward from an implementation perspective, unlike current control which is generally considered challenging.

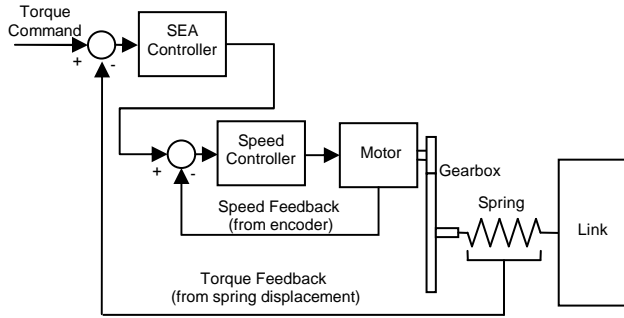


Figure 1: The inner velocity loop in the velocity sourced SEA helps to overcome problems with non-linearities and stiction

2.1 Implementation

We have built a velocity sourced SEA suitable for use in human-robot interaction applications. The design treats the series elastic element as a modular component that might be used with a range of motor systems, as are other transmission elements such as gearboxes. The series elastic element (illustrated in Figure 2) is 120 mm in diameter, and 98.5 mm in length, comprising a body 36 mm long, with 25 mm of output shaft and 37.5 mm of input shaft. Four springs as arranged in the element provide a rotational spring constant of 138 Nm / rad. The springs are always in compression and remain linear in their behaviour.

The deflection sensor is a critical element in the design, as noise or quantisation in the angle measurement impacts system performance dramatically. We have employed a Philips KMZ-41 Magnetic Field Sensor in a 150 kA/m field, achieving an absolute position measurement with 0.01° of resolution.

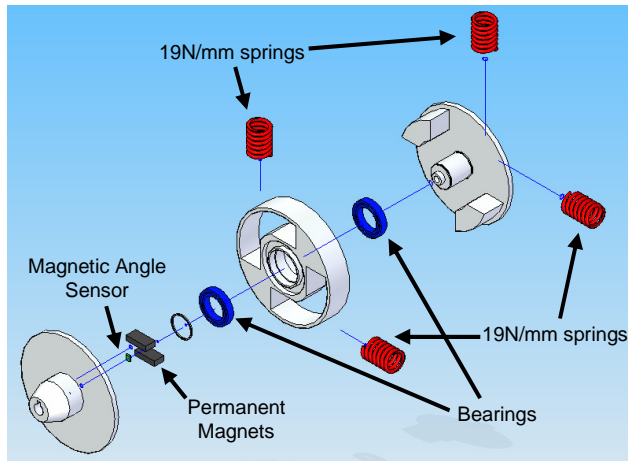


Figure 2: Exploded view of the Series Elastic element used in the Velocity Sourced SEA.

The series elastic element is actuated by a Maxon RE35 90W 42V motor as used in the GuRoo humanoid robot project in our lab. The motor has an integrated GP42C 156:1 planetary gear head and a HED-5540 500CPT encoder. The motor / gear head / encoder has the relevant characteristics listed in Table 1 below.

For these experiments, the element drives a 5 kg link with a moment about the actuator drive axis of 0.6 kg/m². The link has length 0.6 m, representing a typical combined link lengths from the shoulder of an arm used in human-robot interactions. The link is stiff, representing the arm at full stretch, colliding in a direction where the elbow joint has no compliance (for example, orthogonal to the elbow joint's plane of motion).

Table 1: Table of properties of motor used to drive series elastic element.

Nominal Voltage	42 V
Terminal Resistance	2.07 Ω
Terminal Inductance	0.62 mH
Torque Constant	0.0525 Nm/A
Back EMF Constant	0.0525 Vs/rad
Rotor Inertia	6.96 x 10 ⁻⁶ kg.m ²
Reflected Gear Head Inertia	0.91 x 10 ⁻⁶ kg.m ²

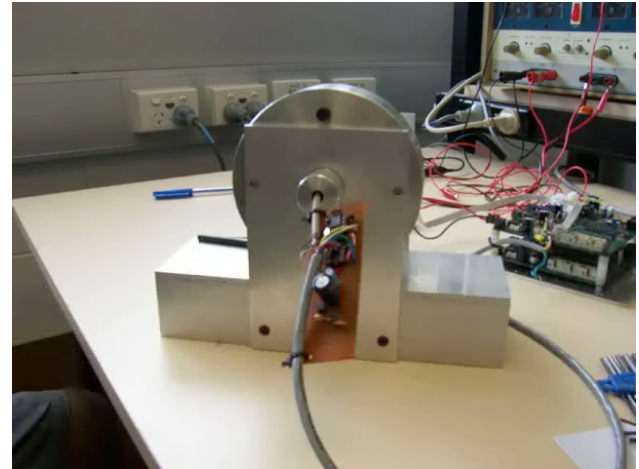


Figure 3: The velocity sourced SEA in its test rig.

Importantly, the power electronics that drive the motor have all current limits removed, allowing large transient currents to quickly actuate the spring to the correct tension for the torque demand. This modification is not intended for protracted steady state high torque applications, but only for the transient torques required to start and stop the actuator moment as it spins quickly to achieve the desired spring tension. Total current is still limited by the motor resistance and the supply voltage to ~20 A peak.

2.2 Control System

The principle of a velocity controlled SEA is shown in Figure 1. The motor has velocity feedback from an encoder that forms a tight loop for controlling the motor and gearbox. The velocity controller is tuned with no load attached, based on the assumption that the spring

decouples any high-frequency torque disturbances on the SEA output, and that a well tuned velocity controller should be able to deal with low-frequency torque disturbances. With this tight velocity control loop in place, the motor can be treated as an effective velocity source, simplifying the ensuing torque control design. However, it is important to note that even in the presence of significant Coulomb and viscous friction losses in the motor and gearbox, a high performance velocity source can still be achieved in this fashion.

2.3 Motor Velocity Controller

The motor velocity controller was tuned for rapid transient response and zero steady state error for a step input. The open loop transfer function (including the electrical pole formed by the motor inductance) is:

$$\frac{\omega_m(s)}{V(s)} = \frac{1.14 \times 10^7}{s^2 + 3339s + 59700}$$

A PI compensator is used to remove steady state error, with a zero at -200. Gain is then chosen to give good response, and to cancel the compensator's zero. With a gain of 0.27, the closed loop transfer function is:

$$\frac{\omega_m(s)}{\omega_d(s)} = \frac{3.192 \times 10^6 (s + 200)}{(s + 202)(s^2 + 3204s + 3.168 \times 10^6)}$$

With close cancellation of the compensator zero, the response is dominated by the complex poles with frequency 1.78 kHz and a damping ratio of 0.88.

2.4 SEA Controller

With the SEA element and 0.6 kg/m² link attached to the motor we can derive the open loop transfer function as:

$$\frac{T_L}{\omega_d} = \frac{1780^2 \cdot 138 / 156 \cdot s}{(s^2 + 3130s + 1780^2)(s^2 + 230)}$$

Using the compensation principle described in our previous work [1], two cascaded PI compensators were used with a gain of 500 to create the closed loop transfer function:

$$\frac{T_L}{T_e} = \frac{1.4 \times 10^9 (s^2 + 40s + 800)}{(s + 1785)(s^2 + 43s + 882)(s^2 + 1302s + 7.1 \times 10^5)}$$

The closed loop system has dominant poles at a frequency of 840 rad/s with a damping ratio of 0.77. The load on the SEA has little impact on the response, although it is fixed for these studies.

The bandwidth is reduced by some of the non-linear effects in the system, particularly the voltage saturation across the motor. The effective bandwidth is closer to 400 rad/s in practice, and as low as 50 rad/s near the torque limit. Further details on the principles and design issues with the controller can be found in [1].

3 Experimental Systems

The purpose of this paper is to quantitatively compare the safety of the velocity-sourced SEA with a similarly specified high-impedance actuator. To this end, a high

impedance form of the actuator has been developed. In order to make meaningful comparisons with the high impedance system, a trajectory controller has been developed for the SEA. Additionally, a collision detection system has been developed for the SEA to evaluate the importance of extrinsic safe reaction in the safe control of low impedance actuators.

3.1 High-Impedance Reference System

For the purposes of comparative study, a high impedance actuator system was implemented based on the same hardware as the Velocity Sourced SEA. This actuator has the SEA element removed, allowing the motor to directly drive the link (see Figure 4).

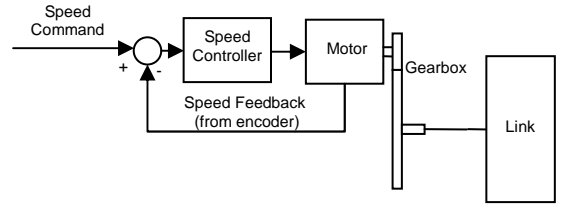


Figure 4: High impedance velocity control system used as reference system for comparison of safety and performance.

In this configuration, the open loop transfer function of the motor is:

$$\frac{\omega_m(s)}{V(s)} = \frac{1.7 \times 10^4}{s^2 + 3339s + 1.4 \times 10^5}$$

With the speed controller implemented with well tuned PI compensation (P = 100, I = 5000) the closed loop transfer function is:

$$\frac{\omega_m(s)}{\omega_d(s)} = \frac{1.69 \times 10^6 (s + 50)}{(s + 2664)(s + 624)(s + 50.8)}$$

Trajectories are generated by supplying a stream of desired velocities at the system sampling rate (3.6 kHz). The nature of the trajectories used is described in the relevant experiments.

3.2 Trajectory Generation for the SEA

In order to compare the low impedance SEA to the high impedance reference system, the SEA requires a further loop to provide velocity based control. For trajectory generation, we borrow from the principles of Virtual Model Control [9]. The trajectory generation system uses a velocity profile command, as used in the high impedance system. The velocity profile is integrated to create a desired angle θ_D for the joint, which is compared to the link angle θ_L derived by summing the angle of the motor θ_M (from the encoder) with the angle of the spring θ_S (from the torque sensor). The VMC controller uses a spring-damper virtual model, with a spring constant K_s of 2000 N / rad and a damper constant K_d of 100 Ns / rad. The torque command to SEA is calculated by:

$$\begin{aligned} \theta_{err} &= \theta_D - (\theta_M + \theta_S) \\ \tau &= K_d \dot{\theta}_{err} + K_s \theta_{err} \end{aligned}$$

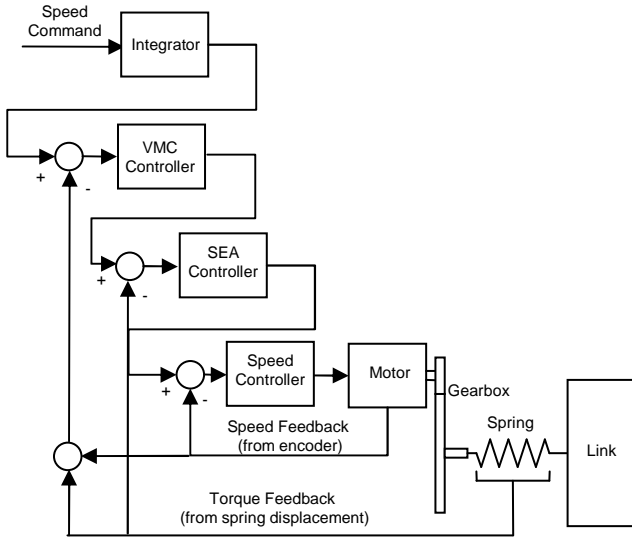


Figure 5: Trajectory generation system for the SEA. The desired position is derived from the input trajectory and compared to the actual link position. A VMC controller generates the torque command for the SEA.

3.3 Collision Detection for the SEA

Safety of the SEA can be potentially further enhanced by implementing a collision detection and safe reaction system into the controller. Collision detection is based on the principles in [10], but simplified for a single degree of freedom.

Collision detection is achieved comparing the momentum of the link as computed from the link's velocity, and the momentum of the link computed from the integral of the torque supplied to the link from the actuator. If the calculations do not match, then the link must have acquired (or lost) momentum due to an external unknown source.

Consider the link operating in a horizontal plane, so that there are no gravity disturbances. The momentum can be derived from two sources.

$$p_L = J_L(\omega_E + \omega_S)$$

$$\dot{p}_L = \tau_S$$

The momentum p_L is calculated from the velocity of the link as measured by derivative of the position information from the encoder, ω_E and spring, ω_S . The rate of change in momentum attributable to the actuator can be derived directly from the measured torque across the spring τ_S . This torque measure should also include any known and expected external torques such as gravity and damping, but in the case of our single joint operating in a horizontal plane there should be no effect from gravity and damping should be negligible.

$$r(t) = K_r \left[p(t) - p(0) - \int_0^t (\tau + r) ds \right]$$

The measure r shows the difference between the two sources of momentum measurement. If r is small then no impact has occurred. If r is above some threshold then

there is impact. The direction of the impact can be determined by looking at the sign of r . If the sign of r is positive then the impact has occurred in the positive direction of motion (the positive direction of ω and τ), else in the negative direction.

The impact measure r is also used in a feedback term to correct any build up of error from the integration process, providing a high pass filter for impact measure. This will correct any small errors in parameter estimation (such as sensor calibration or estimate of J) and will filter slow acting disturbances such as un-modelled friction.

The collision detection system was implemented with a filter gain, K_r , of 10 and a detection threshold, r_{max} , of 0.1. The system reacted to collisions by setting the demand torque to zero, and resetting the integrators in the speed controller and SEA controller to zero.

4 Safety Comparison

The safety of the experimental systems was quantitatively compared by measuring the impact caused by the moving link striking a model of a human head. The safety is assessed for the high impedance actuator, and the Velocity Sourced SEA with and without collision detection.

4.1 Head Injury Criterion

Safety is assessed using the Head Injury Criterion (HIC) [2], a method for assessing the injury probability based on the acceleration of the head during an impact. Despite its comparative simplicity (for example, it does not consider rotational accelerations) the HIC has been shown empirically to be a reliable predictor of intracranial trauma [11]. The HIC is defined as:

$$HIC = \max_{t_2 - t_1 \leq \Delta} \left\{ \left[\frac{1}{t_2 - t_1} \int_{t_1}^{t_2} a(t) dt \right]^{2.5} (t_2 - t_1) \right\}$$

where $a(t)$ is the linear acceleration at centre of the head (notionally the brain) and Δ is a maximum duration set to limit the time extent over which an impact can be considered. The duration Δ was set at 15 ms for following experiments in line for consistency with the Prasad / Mertz injury risk curves [12]. Note that automotive standards set a limit of 750 for HIC (with Δ of 15 ms). An HIC limit of 100 has been quoted as a suitable limit for interactive robots [13].

The Prasad / Mertz injury risk curve plots the probability of head injury for various levels of the Abbreviated Injury Scale (AIS) [3]. The injury types for the three relevant injury scales are listed below:

MAIS 1: Skull trauma without loss of consciousness; fracture of nose or teeth; superficial face injuries.

MAIS 2: Skull trauma with or without dislocated skull fracture and brief loss of consciousness. Fracture of facial bones without dislocation; deep wound(s).

MAIS 4: Cerebral contusion, loss of consciousness for more than 12 hours with intracranial haemorrhaging and other neurological signs; recovery uncertain.

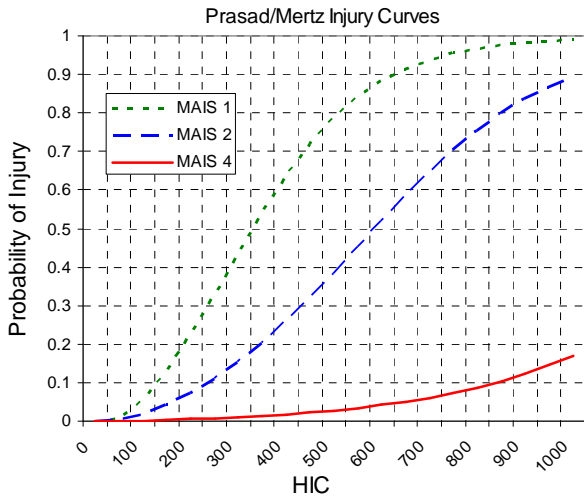


Figure 6: Curve relating the likelihood of various levels of head trauma to HIC value.

4.2 Head Collision Dynamics

The head is modelled as a 5 kg spherical mass on a low friction surface with a firm, elastic covering. Collisions occur normal to the surface of the head and parallel to the low friction surface. The covering has a spring constant of 10 kN/m. The 5kg link with a moment about the actuator drive axis of 0.6 kg/m² strikes the head at 500 mm along the link's length.

The link is accelerated from rest at constant acceleration for 0.5 s and then maintains a constant velocity. The mass is positioned so that the collision will occur 0.75 s after the link starts moving. For the purposes of comparison, results are also obtained for a free swinging link with no actuator at all, having the same mass distribution, and moving at the same speed at impact. The constants used in the trajectories are listed in Table 2.

Table 2: Trajectory constants used for testing profiles.

Collision Speed	Profile Acceleration	Angle from Start Position
0.5 m/s	2 rad/s ²	0.5 rad
1.0 m/s	4 rad/s ²	1.0 rad
1.5 m/s	6 rad/s ²	1.5 rad

4.3 Safety Results

The graphs below (Figure 7, Figure 8 and Figure 9) show the results of the head impact tests. The SEA is shown to have consistently the best safety performance of the actuated systems. With the collision detection system in operation, the SEA is comparable to a completely unactuated link, with both HIC and peak acceleration results at similar values to the unactuated system. The observation applies across the entire range of experimental collision speeds.

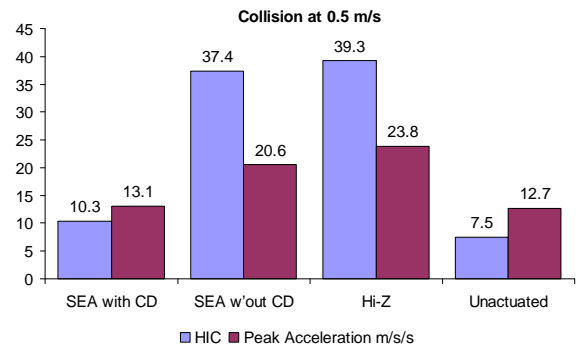


Figure 7: Graph of head collision results showing the comparison between the tested systems in terms of HIC and peak head acceleration for a collision at 0.5 m/s.

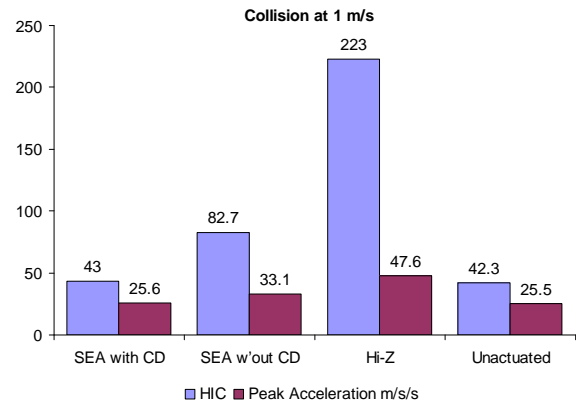


Figure 8: Graph of head collision results showing the comparison between the tested systems in terms of HIC and peak head acceleration for a collision at 1 m/s.

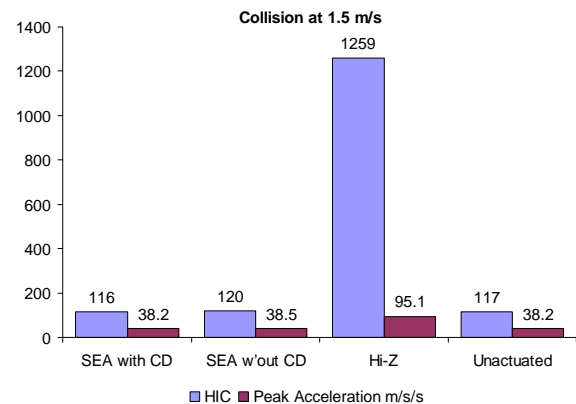


Figure 9: Graph of head collision results showing the comparison between the tested systems in terms of HIC and peak head acceleration for a collision at 1.5 m/s.

Surprisingly, the SEA without collision detection performs quite poorly when at lower speeds. When no collision detection is enabled, the SEA initially bounces from the head but then strikes it a second time as the VMC controller loop acts to maintain the desired joint angle. This effect is illustrated in the comparative acceleration profiles shown in Figure 10. However, at these low speeds, none of the systems is likely to cause a head injury of any description.

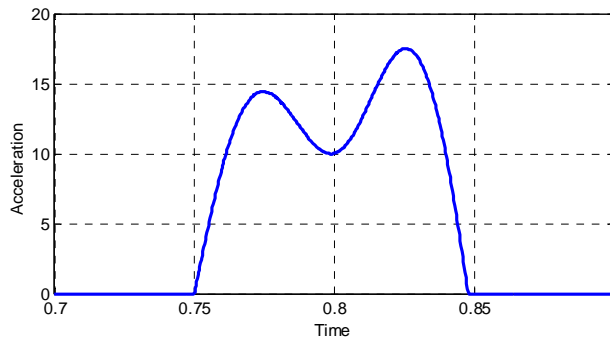


Figure 10: Acceleration profile of head from SEA with collision detection disabled for a collision at 0.5 m/s.

At higher speeds, the HIC values associated with the SEA using collision detection and the unactuated link are very unlikely to produce a critical injury (MAIS 4), and have low probability of causing any injury at all (less than 8%). The high impedance arm is almost certain to produce an injury requiring hospitalisation, and has a 35% chance of causing a head injury that will lead to death or permanent injury. Clearly the SEA has extended the safe performance range of the arm, allowing much greater actuation speeds than a stiff actuator can safely provide.

Table 3: Table of likely injury outcomes for each of the experimental systems for collisions at 1.5 m/s.

System	MAIS 1	MAIS 2	MAIS 4
SEA with CD	8%	3%	0%
SEA w'out CD	8%	3%	0%
Hi-Z	100%	97%	35%
Unactuated	8%	3%	0%

5 Conclusions

The Velocity Sourced Series Elastic Actuator has significant intrinsic safety advantages over similarly specified actuators with no elastic component. At speeds where a high impedance actuator has a 97% chance of causing serious head injury, the Velocity Sourced SEA has only a 3% chance of causing the same level of injury. Collision detection and safe reaction can improve comfort at low speeds, but seems unlikely to improve the overall safe operation of the actuator with respect to any form of assessable injury.

5.1 Future Work

There remain several issues for ongoing investigation. In achieving both high performance and high safety from the SEA, there has been a compromise in power consumption. The motor drive requires novel power electronics to capture energy that is unnecessarily thrown away when the armature is spun up and then down during torque level transitions. In addition, the design of trajectories that minimise angular jerk will also improve power economy and tracking performance. Finally, we

hope to perform a more complete set of safety experiments using a manipulator with more degrees of freedom, and an instrumented test dummy.

References

- [1] G. Wyeth, "Control Issues for Velocity Sourced Series Elastic Actuators," presented at Australasian Conference on Robotics and Automation (ACRA 2006), Auckland, 2006.
- [2] J. Newman, "Head injury criteria in automotive crash testing," presented at 24th Stapp Car Crash Conference, 1980.
- [3] -, *Abbreviated Injury Scale (AIS) 2005 Manual*: Association of the Advancement of Automotive Medicine Publications, 2005.
- [4] G. A. Pratt and M. M. Williamson, "Series Elastic Actuators," presented at International Conference on Robotic Systems (IROS), 1995.
- [5] M. M. Williamson, "Series Elastic Actuators," in *Department of Electrical Engineering and Computer Science*. Boston: Massachusetts Institute of Technology, 1995.
- [6] D. W. Robinson, J. E. Pratt, D. J. Paluska, and G. A. Pratt, "Series Elastic Actuator Development for a Biomimetic Walking Robot," presented at IEEE/ASME Int'l Conf. On Adv. Intelligent Mechatronics, 1999.
- [7] G. A. Pratt, P. Willisson, C. Bolton, and A. Hofman, "Late Motor Processing in Low-Impedance Robots: Impedance Control of Series Elastic Actuators," presented at Proc of American Control Conference, Boston, MA, 2004.
- [8] D. W. Robinson, "Design and Analysis of Series Elasticity in Closed-loop Actuator Force Control," in *Department of Mechanical Engineering*: Massachusetts Institute of Technology, 2000.
- [9] J. E. Pratt, C.-M. Chew, A. Torres, and G. Pratt, "Virtual Model Control: An Intuitive Approach for Bipedal Locomotion," *The International Journal of Robotics Research*, pp. 129-143, 2001.
- [10] A. De Luca, A. Albu-Schaffer, S. Haddadin, and G. Hirzinger, "Collision Detection and Safe Reaction with the DLR-III Lightweight Manipulator Arm," presented at International Conference on Intelligent Robots and Systems, Beijing, China, 2006.
- [11] F. J. Lockett, "Biomechanics justification for empirical head tolerance criteria," *J. Biomechanics*, vol. 18, pp. 217-224, 1985.
- [12] P. Prasad and H. Mertz, "The position of the United States delegation to the ISO working group 6b on the use of HIC in the automotive environment," SAE Paper 821246, 1982.
- [13] A. Bicchi and G. Tonietti, "Fast and "Soft-Arm" Tactics: Dealing with the Safety-Performance Tradeoff in Robot Arms Design and Control," *IEEE Robotics & Automation Magazine*, pp. 22-33, 2004.